Stability and instability in the anisotropic Kepler problem

2005 J. Phys. A: Math. Gen. 38 8897

(http://iopscience.iop.org/0305-4470/38/41/005)

INSTITUTE OF PHYSICS PUBLISHING JOURNAL OF PHYSICS A: MATHEMATICAL AND GENERAL

J. Phys. A: Math. Gen. **38** (2005) 8897–8920 doi:10.1088/0305-4470/38/41/005

Stability and instability in the anisotropic Kepler problem

G Contopoulos and M Harsoula

Research Center for Astronomy, Academy of Athens, Soranou Efessiou 4, GR-11527, Athens, Greece

Received 14 July 2005, in final form 31 August 2005
Published 28 September 2005
Online at stacks.iop.org/JPhysA/38/8897

Abstract

We study the degree of order and chaos in the anisotropic Kepler problem. The Lyapunov characteristic number (LCN) is constant for all orbits in the chaotic domain with a fixed mass ratio μ. It increases from zero as the mass ratio μ increases from $\mu = 1$, reaches a maximum for $\mu = 4$ and then decreases slowly to zero for a very large μ. We found the characteristics of many families of the periodic orbits of multiplicities up to 17. Several families have a stable part for μ close to $\mu = 1$ (namely, $\mu < 1.748$). We conjecture that there are stable orbits of high multiplicities for larger values of μ. The stable orbits are surrounded by islands of stability consisting of closed invariant curves. The rotation number along these invariant curves decreases from the periodic orbits outwards. Higher-order islands are enclosed in every main island around a low-order periodic orbit. In the case $\mu = 1.1$, we find a large number of islands of multiplicities from 3 up to 17. Then we calculate the asymptotic curves from unstable periodic orbits. These curves go through the collision orbits but continue beyond these points. The intersections of the stable and unstable asymptotic curves are homoclinic and heteroclinic points. The corresponding orbits are the main characteristics of chaos.

PACS number: 95.10.–a

1. Introduction

The anisotropic Kepler problem (AKP) was introduced by Gutzwiller (1967, 1969, 1970, 1971, 1977, 1989, 1990) as a possible example of 'hard chaos', i.e., a system without stable periodic orbits. Thus the anisotropic Kepler problem was considered as a candidate Anosov system. (The definitions of some terms used in the present paper, such as Anosov and Bernoulli systems, etc can be found in the appendix). Gutzwiller (1977) and Devaney (1978a,1978b) found an approximate correspondence between this system and a Bernoulli system.

It is remarkable that no Hamiltonian Anosov system has been found up to now. The 'best' candidate for an Anosov system was the Yang–Mills system (Savvidy 1983), but the claim that this system is Anosov was disproved by the discovery of an island of stability (Dahlquist and Russberg 1990). Only systems with abrupt reflections, such as the stadium (Bunimovich and Sinai 1980), the rational billiards (Eckhardt *et al* 1984), and similar systems, are known to be Anosov. But as soon as smoothness is introduced to avoid the abrupt reflections, islands of stability appear and the systems are not even ergodic. Thus the possibility that the anisotropic Kepler problem is Anosov generated a large interest in it.

However, Broucke (1985) found two stable periodic orbits of periods 3 and 5, surrounded by islands of stability for a mass ratio near $\mu = 1.5$. Therefore the AKP system is neither Anosov nor Bernoulli.

But the Broucke islands disappear for larger values of μ ($\mu > 1.748$). Thus Gutzwiller (1990) conjectured that for mass ratios $\mu > 2$, no stable periodic orbits exist and hard chaos persists for large μ.

In the present paper, we describe several families of stable orbits that exist for $\mu < 1.748$. We conjecture that higher-order stable orbits exist for an arbitrarily large μ. This is analogous to a theorem due to Duarte (1994) for the standard map. On the other hand, an Anosov system is structurally stable, i.e., a small perturbation of it continues to be an Anosov system. Therefore if our conjecture is correct the AKP cannot be an Anosov system even for large μ.

Most of the studies of the anisotropic Kepler problem have been made for mass ratios $\mu > 9/8$. In fact the topology of the collision orbits changes when μ crosses the value $\mu = 9/8$ (Devaney 1978b). Although extensive studies of the AKP have been made (Casasayas and Llibre 1984, Gutzwiller 1990), very little has been done for the cases $1 < \mu < 9/8$. Casasayas and Llibre (1984) claim that for $\mu < 9/8$ the AKP is not chaotic. However, in a recent paper, Bai and Zheng (2002) have shown that the AKP is chaotic even for μ slightly above 1. This is due to the fact that the perturbation for μ slightly larger than 1 is large when a particle approaches the origin.

This conclusion is established in the present paper by calculating the LCN of many chaotic orbits for various values of μ. For such orbits, LCN is positive for all values of μ larger than 1, and therefore the anisotropic Kepler problem is chaotic for all $\mu > 1$.

The paper is organized as follows. In section 2, we describe various forms of the equations of motion. In section 3, we calculate the Lyapunov characteristic numbers. In section 4, we describe the various families of periodic orbits. We find their characteristics (x versus μ) and their stability diagrams (a versus μ). In section 5, we describe the islands of stability and calculate their overall size. In section 6, we find the rotation numbers of various islands of stability. In section 7, we calculate the asymptotic curves of the unstable periodic orbits and their intersections. Finally, in section 8, we summarize our conclusions.

2. Equations of motion

In the notation of Broucke (1985) the Hamiltonian of the anisotropic Kepler problem is

$$H_B = \tfrac{1}{2}\left(\dot{x}_B^2 + \dot{y}_B^2\right) - \left(\mu_B x_B^2 + y_B^2\right)^{-1/2}. \tag{1}$$

This Hamiltonian is also used by Casasayas and Llibre (1984). In this case the heavy axis for $\mu_B > 1$ is $x_B = 0$, i.e. the force towards the y_B-axis ($x_B = 0$) is stronger than the force towards the x_B-axis.

In the notation of Gutzwiller (1990) the Hamiltonian is

$$H_G = \frac{1}{2}\left(\frac{U_G^2}{\mu_G} + \frac{V_G^2}{\nu_G}\right) - \left(x_G^2 + y_G^2\right)^{-1/2} = \frac{1}{2}\left(\mu_G \dot{x}_G^2 + \nu_G \dot{y}_G^2\right) - \left(x_G^2 + y_G^2\right)^{-1/2}, \tag{2}$$

where

$$U_G = \mu_G \dot{x}_G, \qquad V_G = \nu_G \dot{y}_G \tag{3}$$

and

$$\mu_G \nu_G = 1. \tag{4}$$

In this case the heavy axis for $\mu_G > 1$ is $y_G = 0$. The mass ratio is the quantity $\mu_G/\nu_G = \mu_G^2$.

The relations between the two notations are as follows:

$$H_B = \mu_G^{1/3} H_G \tag{5}$$

and

$$\mu_B = \mu_G^{-2}. \tag{6}$$

Therefore

$$x_B = \mu_G^{2/3} x_G, \qquad y_B = \mu_G^{-1/3} y_G. \tag{7}$$

The basic difference between the two notations is that the anisotropy is introduced in the potential in the Broucke notation, while it is introduced in the kinetic energy in the Gutzwiller notation.

In the present paper, we use a slightly simplified version of the Gutzwiller notation, namely

$$H = \mu_G^{1/3} H_G = \frac{1}{2}\left(\frac{u^2}{\mu} + v^2\right) - (x^2 + y^2)^{-1/2} = \frac{1}{2}(\mu \dot{x}^2 + \dot{y}^2) - (x^2 + y^2)^{-1/2} \tag{8}$$

with

$$\mu = \frac{\mu_G}{\nu_G} = \mu_G^2 \tag{9}$$

and

$$x = \mu_G^{-1/3} x_G, \qquad y = \mu_G^{-1/3} y_G, \qquad u = \mu_G^{2/3} U_G, \qquad v = \mu_G^{2/3} V_G. \tag{10}$$

Therefore μ is equal to the mass ratio μ_G^2, and μ_B is its inverse $1/\mu$.

Devaney (1978b) uses a form similar to equation (8) but with μ replaced by $1/\mu$. This corresponds to an interchange of x and y (Broucke 1985).

In the following, we use a surface of section $y = 0$. On this surface we introduce also X and U variables similar to those of Gutzwiller, namely

$$X = x\left(1 + \frac{u^2}{\mu}\right), \qquad U = \frac{2}{\pi} \tan^{-1}\left(\frac{u}{\sqrt{\mu}}\right); \tag{11}$$

Gutzwiller (1990) uses similar formulae with x_G, U_G, and μ_G.

In a way similar to Gutzwiller (1990) we take $H = -1/2$. Then from equation (8) we find $|x| \leqslant 2$ and $|X| \leqslant 2$, i.e. X varies from -2 to $+2$. At the same time the value of U varies from -1 to $+1$. The values $U = \pm 1$ are reached when u tends to $\pm\infty$. In these cases x tends to zero, i.e., we have collision orbits ($x = y = 0$). Then X can take any value from -2 to $+2$. However, the theoretical studies of Gutzwiller (1977), Devaney (1978b), Casasayas and Llibre (1984) and Broucke (1985) have shown that for $U = \pm 1$, X takes only particular values. These values will be discussed in section 7.

In the Hamiltonian (8) we have calculated many orbits with initial conditions on the $y = 0$ axis with positive $\dot{y}$, derived from the energy equation (8). As integration step we have used the value $\Delta t = 10^{-4}\,(x^2 + y^2)^{1/2}$. Therefore this step decreases and tends to zero if the orbit approaches the origin $x = y = 0$. But sometimes even smaller steps are necessary.

In particular, we have calculated the periodic orbits that intersect the x-axis perpendicularly, i.e. with $\dot{x} = 0$.

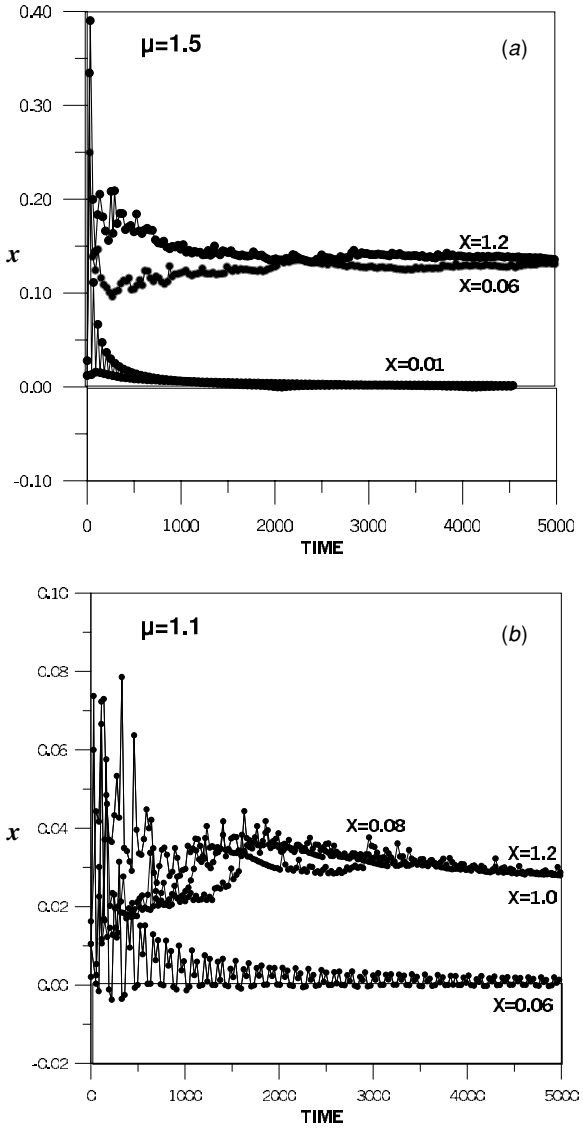

Figure 1. The values of the finite time LCN for various orbits with given initial conditions x and $\dot{x} = 0$; (a) $\mu = 1.5$, (b) $\mu = 1.1$.

3. Lyapunov characteristic numbers

We calculated many orbits of the anisotropic Kepler problem for various values of μ and found the Lyapunov characteristic number which is the limit of the quantity

$$\chi = \frac{\ln(\xi/\xi_0)}{t} \tag{12}$$

for $t \to \infty$, where ξ_0 and ξ are the measures of infinitesimal deviations from the points of a given orbit for $t = 0$ and for any given t, respectively. The quantity χ is a 'finite time LCN'. Two typical examples are given in figures 1(a) and (b) for $\mu = 1.5$ and $\mu = 1.1$. We see

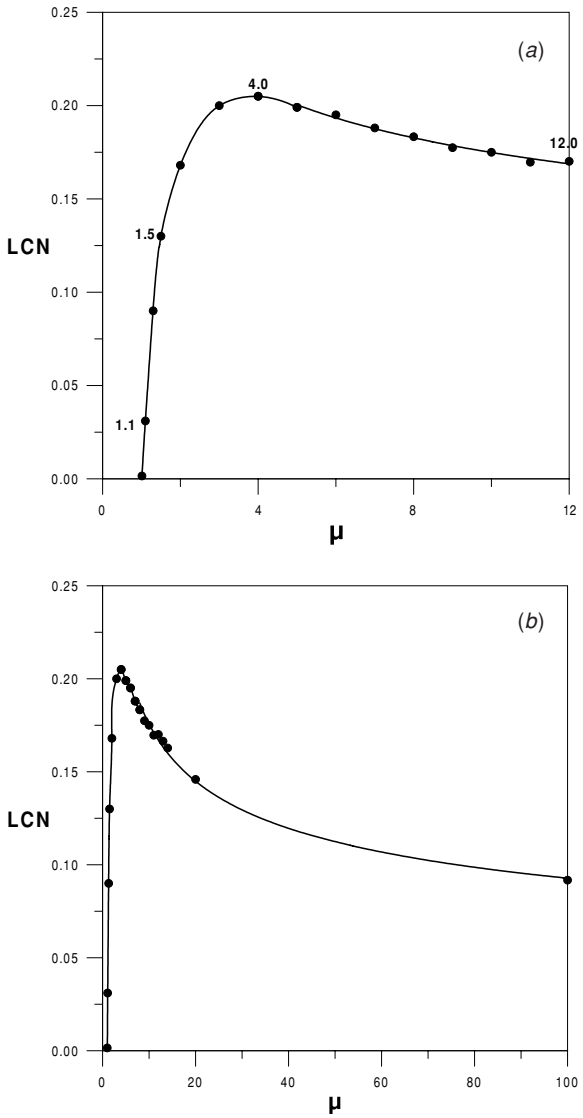

Figure 2. The LCN of chaotic orbits as a function of the mass ratio μ. (*a*) Up to $\mu = 12$ and (*b*) up to $\mu = 100$.

that the 'finite time LCN' may have large variations for small times, but as t increases the variations become smaller.

The 'finite time LCN' tends to the LCN as $t \to \infty$. This is zero inside the islands of stability and a fixed positive number in the chaotic domain for fixed μ. This number is a function of μ only (figures 2(*a*) and (*b*)).

In the case of the Kepler problem ($\mu = 1$) the LCN is always zero, but for all $\mu > 1$ the LCN for most orbits is positive. It increases when μ increases from $\mu = 1$ to $\mu = 4$ (figure 2(*a*)), reaching a maximum value LCN ≈ 0.21. For a larger μ, the LCN gradually decreases to LCN $=$ 0.09 for $\mu = 100$.

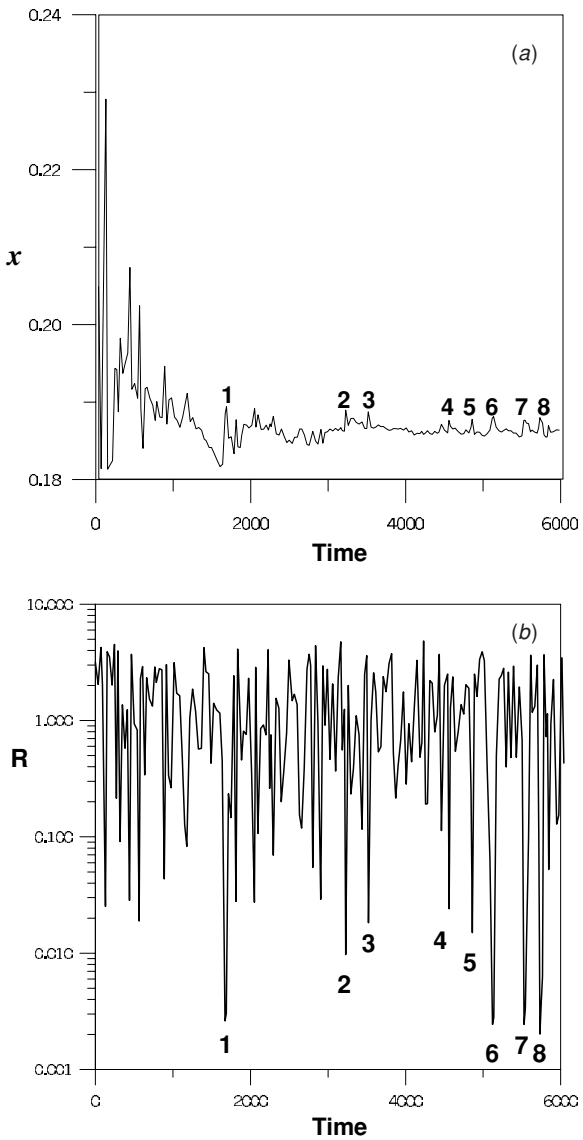

Figure 3. (*a*) The finite time LCN χ and (*b*) the distance R from the centre as a function of time along an orbit with $\mu = 7$ and $x = 1.2$, $\dot{x} = y = 0$.

Therefore the anisotropic Kepler problem is chaotic for all values of $\mu > 1$. This chaotic behaviour is not due only to collisions, as has been claimed. In fact when a chaotic orbit approaches the origin ($x = y = 0$), the value of χ becomes temporarily large. But later on, it comes back to its long-term value which is positive, both close and far from the origin. This is seen in figures 3(*a*) and (*b*), where we compare the values of χ (figure 3(*a*)) with the values of the distance $R = (x^2 + y^2)^{1/2}$ from the centre along an orbit. The value of R becomes temporarily very small at the points $1, 2, \ldots, 8$. At the same times we see temporarily peaks in the value of χ as a function of time.

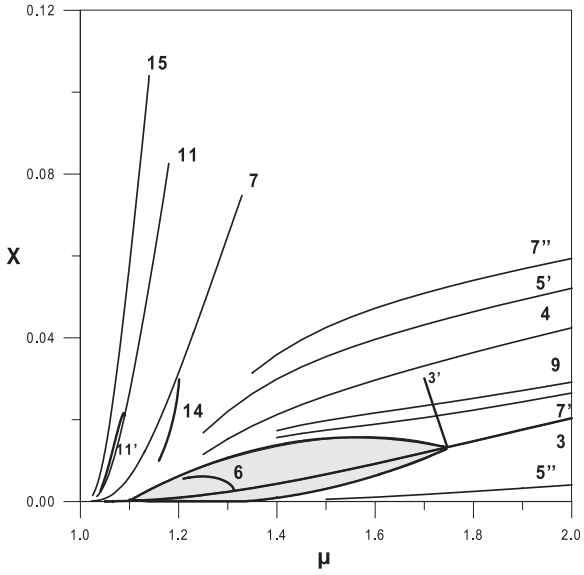

Figure 4. The characteristics (x versus μ) of several families of periodic orbits intersecting perpendicularly the x-axis. Families 3, 6, 5′, 5″, 7, 7′, 7″, 9, 11, 11′, 15 have some stable parts. We mark the stability region around the central point of family 3 (close to (0, 0)).

It seems probable that LCN tends to zero as μ tends to infinity, because then the motions tend to be confined on the x-axis, i.e., the problem tends to become one-dimensional and such problems are integrable.

4. Periodic orbits

In figure 4 we give the characteristics of several families of periodic orbits of multiplicity (number of crossings of the x-axis with $\dot{y} > 0$) $m = 3, 4, 5', 5'' 7, 7', 7'', 9, 11$ and 15, and also families $3'$ and 6, bifurcating from family 3, family 14 bifurcating from family 7, and family $11'$ bifurcating from family 11 (primes refer to different families of the same multiplicity). These orbits intersect the x-axis perpendicularly, i.e. with $\dot{x} = 0$, and they are symmetric with respect to the x-axis.

In order to find periodic orbits with $\dot{x} = 0$, we calculate orbits with initial conditions x, and $y = \dot{x} = 0$ ($\dot{y} > 0$) up to the mth intersection, proceeding with a small step Δx. If two successive orbits have $\dot{x}_f$'s of opposite sign at their final points, then we find a periodic orbit with $\dot{x}_f = 0$ by successive interpolations.

All these families tend to the limit $x = 0$ when μ decreases and tends to 1. In particular, the x-coordinate of family $5''$ for $\dot{x} = 0$ is very close to the origin $x = 0$, closer than family 3. On the other hand, there are further families that tend to finite values of x for $\mu \to 1$. Such is family 1 (figure 5) that tends to a circular orbit with $x = 1$ for $\mu \to 1$, and families like $3''$, 5 and $7'''$ that tend to $x = 2$ (at the boundary of the permissible phase space) as $\mu \to 1$.

The characteristic of family 7 in figure 5 contains a continuation of the same characteristic of figure 4, but for larger values of μ. We see that x increases up to a maximum $x_{\max} \approx 0.34$ for $\mu \approx 4$ and then x gradually decreases.

In figure 6(a) we give the Hénon (1965) stability parameter a along the various families. The families are stable if $-1 < a < 1$ and unstable if $|a| > 1$.

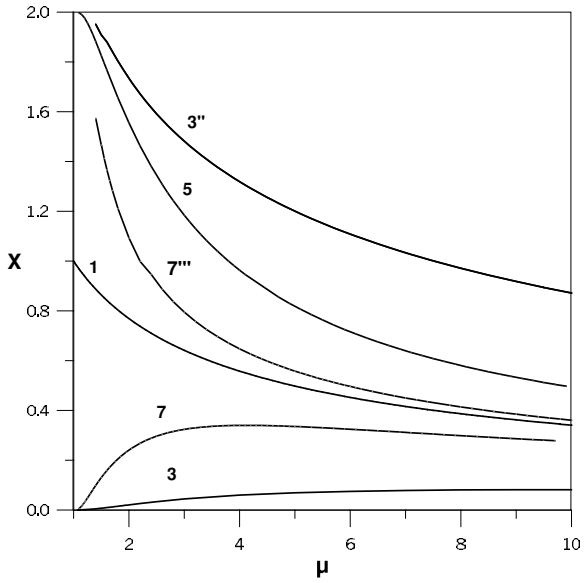

Figure 5. The characteristics (x versus μ) of the families 3, 7, 1, $7'''$, 5 and $3''$. When μ tends to 1, Families 3 and 7 tend to $x = 0$, family 1 tends to $x = 1$ and families $3''$, 5 and $7'''$ tend to $x = 2$.

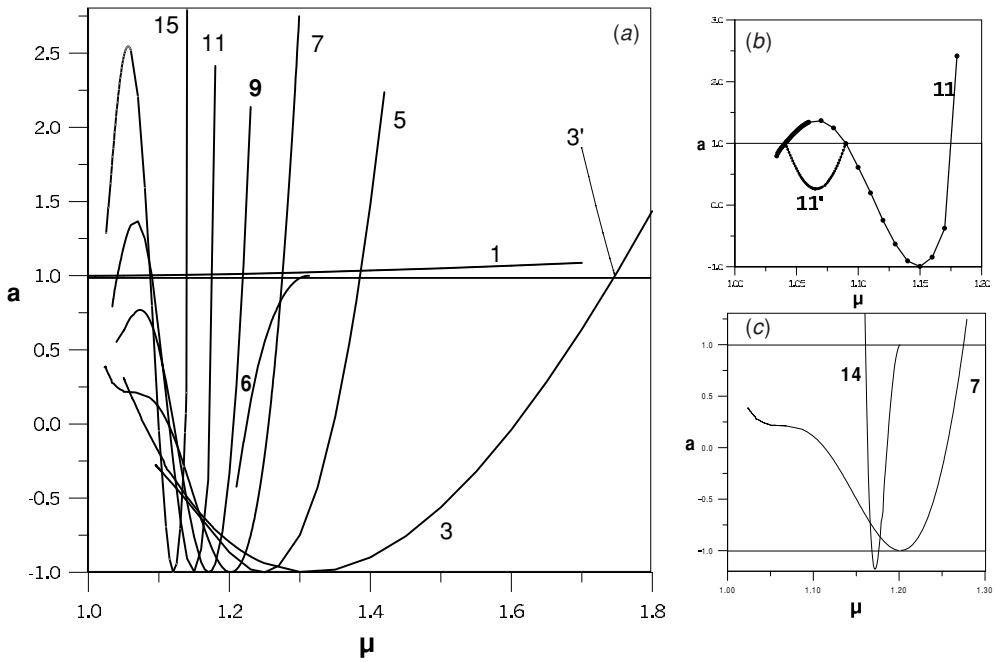

Figure 6. Stability curves (a versus μ) of various families. (a) Families 1, 3, $3'$, 5, 6, 7, 9, 11 and 15. All these families except families 1 and $3'$, have stable parts for an interval of values of μ. (b) The stability curves of the families 11 and $11'$. (c) The stability curves of families 7 and 14.

We notice that families 3, 5, 7, 9, 11, 15 (we call them 'main families' in contrast with the 'bifurcating families') and the bifurcating families 6, $11'$ and 14 are stable in an interval of

values of μ. In particular, family 3 has the largest stable interval, from $\mu = 1$ to $\mu = 1.748$. All the stability curves of the main families touch the line $a = -1$ but never reach values of a smaller than $a = -1$. At the tangent points these families generate other families of double period by period doubling bifurcations, that start at the same μ but with $a = 1$ and are directed towards smaller values of μ and $a < 1$. In particular, family 3 in figure 6 generates the stable family 6 (figure 6(*a*)) and the family 7 generates the stable family 14 (figure 6(*c*)). Family $11'$ (figure 6(*b*)) joins two bifurcation points of family 11 and is everywhere stable. On the other hand, family 14 (figure 6(*c*)) has a stable part from $a = 1$ to $a = -1$, then an unstable part below $a = -1$, and a second stable part from $a = -1$ to $a = 1$, and for smaller values of μ this family becomes unstable with $a > 1$.

On the other hand, at the maximum values of μ where the characteristics cross the axis $a = 1$ we have the bifurcation of unstable families of the same multiplicity that are directed towards smaller μ. This is seen in figure 6 in the case of family 3. The unstable family $3'$ that bifurcates from family 3 at $\mu = 1.748$ has two branches asymmetric with respect to the x-axis, but symmetric with respect to each other.

Similar bifurcations of families of equal period (equal multiplicity) appear at the maximum values of μ, where these families become unstable from stable. The bifurcating families are unstable and exist for μ smaller than the maximum values of μ.

Families 11 and 15 become unstable ($a > 1$) as μ decreases, but as μ decreases further, the values of a reach a maximum $a_{\max}$, and then decrease and become again smaller than 1, i.e. these families become again stable for values of μ close to $\mu = 1$. At the two smaller values of μ where the stability curve 11 crosses the line $a = 1$ we have the bifurcation of a stable family $11'$ (figure 6(*b*)) that joins these bifurcation points. The same joining happens with family $15'$ that bifurcates from two points of family 15 that have $a = 1$.

Family 1 is everywhere slightly unstable (figure 6) for all $\mu > 1$. Its stability parameter a grows slightly from $a = 1$ at $\mu = 1$, as μ increases.

The stability curves of families 3, 5, 7 seem to tend to $a = 1$ when μ tends to 1. In particular, the stability curve of family 7 has a strange inflection point near $\mu = 1.07$. On the other hand, there are several families that are completely unstable with large values of a. Such are families $3''$ and $7''$ (figure 7). They have a very large a for small μ (>1), then reach a minimum a (>1) as μ increases, and as μ increases further a increases to very large values. In these cases when μ tends to 1, the stability index α tends probably to infinity. However, there are also cases in which the stability index for $\mu \to 1$ is smaller than $a = 1$, perhaps reaching the value $a = -1$. Such are families 9, 11 and 15.

The forms of the various types of periodic orbits up to multiplicity 5 have been described in detail by Gutzwiller (1982).

Here we give only one example of a triple periodic orbit (figure 8(*a*)) of the Broucke (1985) type. This orbit consists of two almost straight line segments joined by a small loop around the origin (0, 0). As μ decreases and tends to 1, the size of the loop decreases and tends to one point. Thus the limit of the Broucke orbit 3 is a couple of straight line orbits from $\mu = 1$, which are then independent of each other. As μ increases the size of the loop increases. In figure 8(*b*) we give, for comparison, the loop of this orbit for $\mu = 2.5$, which is much larger.

5. Islands of stability

The islands of stability surround stable periodic orbits. An example is the three islands of stability (figures 9 and 10) around the periodic orbit 3 on the surface of section (X, U) (i.e. $y = 0$, with $\dot{y} > 0$). The stable periodic orbit is represented by 3 points at the centres of the

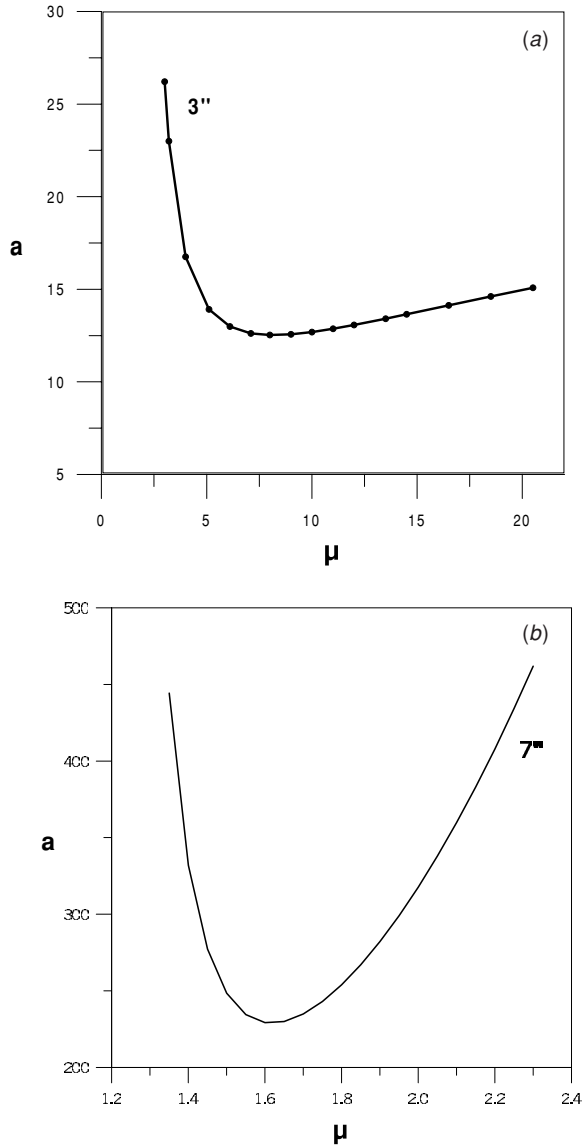

Figure 7. Stability curves of families $3''$ and $7''$ that never become stable.

islands. These points are surrounded by closed invariant curves, but outside the islands there is chaos.

The size of the islands around the periodic orbit 3 of figure 9 (close to the origin (0, 0)) is shown in figure 4 for $\mu = 1.5$. The maximum size appears in the region $\mu = 1.4$–1.5. For larger and for smaller μ the sizes are smaller. In figures 9 and 10 we give the three islands for $\mu = 1.5$ (one island in figure 9 and two symmetric islands in figure 10). In the inserts of figure 9 and in figure 10 we give also the islands for $\mu = 1.745$ (close to the maximum value of μ which corresponds to a stable orbit 3) and for $\mu = 1.1$. In both cases the islands are very thin.

In the cases $\mu < 1.32$ inside the main islands of period 3 there are four secondary islands corresponding to two stable bifurcating families 6 (figure 11(*a*) for $\mu = 1.3$). We have also

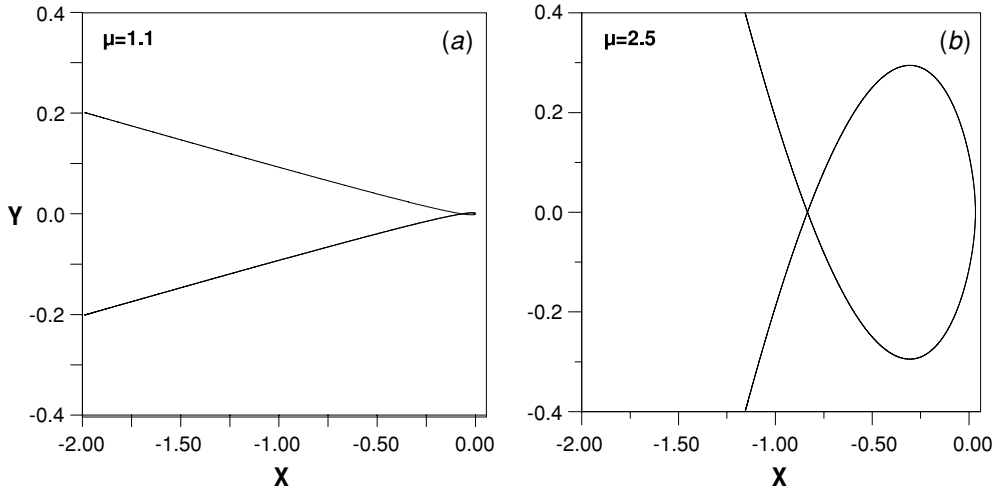

Figure 8. (*a*) A triple periodic orbit for $\mu = 1.1$. (*b*) The loop of the triple orbit for $\mu = 2.5$.

two unstable bifurcating families 6 between the stable families. In figure 11(*b*) we see that island 3 extends well beyond the curves of figure 11(*a*).

Similar, but smaller, islands appear near other stable periodic orbits. For example, in figure 12 we see three islands around 3 stable points of the family 5 for $\mu = 1.2$. Each of these islands is surrounded by four secondary islands corresponding to two stable period 10 families, which have bifurcated from the period 5 family. There are also two unstable period 10 families between the stable period 10 families.

A large number of islands of multiplicities from 3 to 17 are found in the case $\mu = 1.1$ (figure 13).

6. Rotation numbers

One way to find the bifurcations from a given stable family is by calculating the rotation number of various invariant curves around the central point. This is the average angle between the directions of successive intersections of the surface of section by an orbit, as seen from the periodic orbit (central point) with the circle as unity.

In figure 14 we calculated the rotation curves, i.e. the rotation numbers as functions of x, for a few values of μ. For $\mu = 1.5$, the rotation curve has its maximum Rot ≈ 0.34 at the central point x ≈ 0.008, which is the periodic orbit. Rot decreases outwards and tends to zero at the limit of the island. Whenever Rot goes through a rational value we have a bifurcated higher-order family.

In figure 14 we see that the simplest rational Rot of a bifurcated family for $\mu = 1.5$ is Rot $= 1/3$, i.e. the corresponding bifurcated family has a period 3 times the period of the original family, i.e. period 9. This family appears very close to the central periodic orbit.

For $\mu = 1.3$, the rotation curve goes above Rot $= 1/2$. Therefore we have a bifurcated family of period 2 times the period of the original family 3, i.e. its period is 6. In fact we have two period 6 families, one with $\dot{x} = 0$ and one with $\dot{x} \neq 0$ (figure 11(*a*)). The island of period 6 on the right extends from $x = 0.0039$ to $x = 0.0053$. In this interval the corresponding rotation curve for $\mu = 1.3$ (figure 14) has a small horizontal part. The curve $\mu = 1.3$ continues with

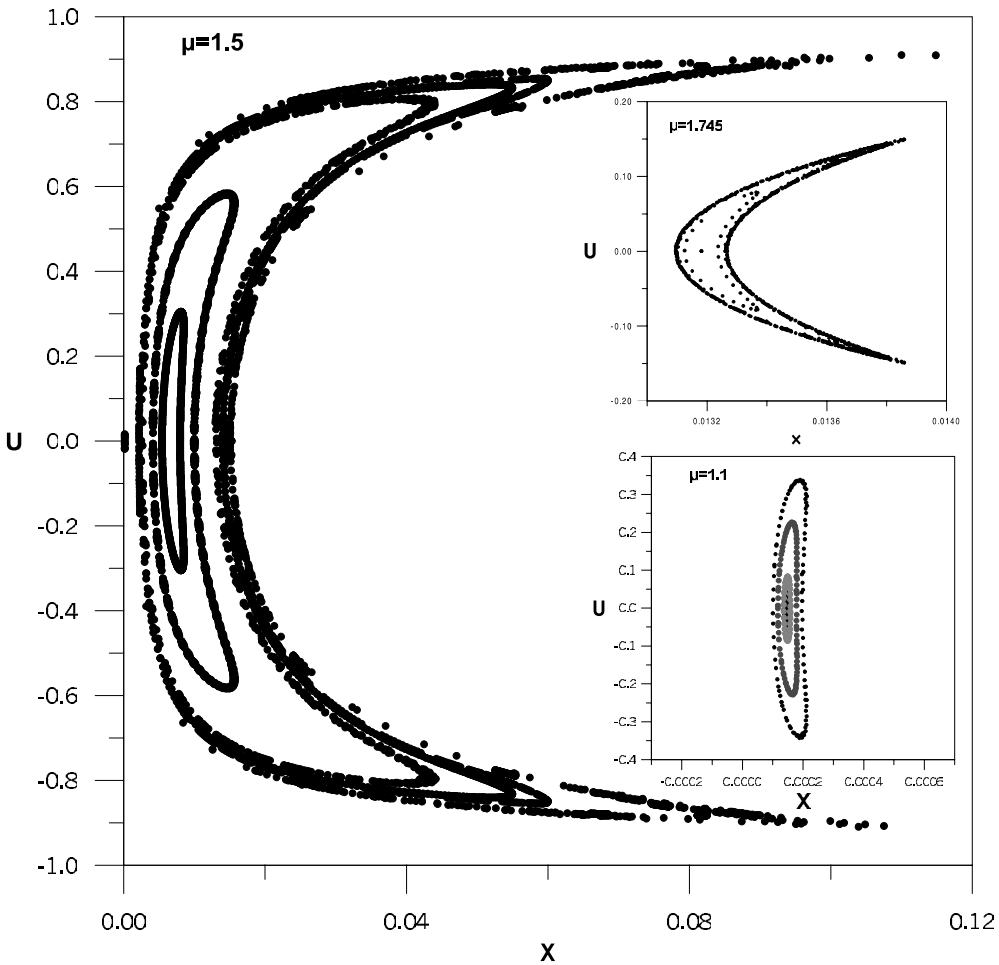

Figure 9. An island of stability around the stable point on the x-axis close to $x = X = 0$ that represents the period-3 orbit for $\mu = 1.5$. The central point is surrounded by closed invariant curves. We mark also the thin islands of the same type for $\mu = 1.1$ and $\mu = 1.745$. The axes are X and U of equation (11).

smaller values of Rot beyond island 6. It has a smaller horizontal part with Rot $= 2/5$ near $x = 0.010$ and beyond that Rot decreases to zero at the boundary of the island. In fact island 3 extends up to about $x = 0.012$ on the axis $\dot{x} = 0$ (figure 11(b)).

As μ increases the maximum Rot decreases. This can be seen in figure 14, where we compare the rotation curves for $\mu = 1.1$, $\mu = 1.3$, $\mu = 1.5$ and $\mu = 1.7$. In the case $\mu = 1.1$, the maximum Rot is $\approx$0.72 for $x \approx 0.0002$ and for larger x the value of Rot goes very fast to zero. For $\mu = 1.3$, the maximum Rot is $\approx$0.51 for $x \approx 0.0023$, and for $\mu = 1.7$ the maximum Rot is $\approx$0.14 at $x \approx 0.0122$, and for larger x the value of Rot goes rather fast to zero.

In figure 15(b) we see a similar rotation curve for the stable family 7 and $\mu = 1.2$, that gives Rot as a function of x along the line $U = 0$ in figure 15(a). This line crosses the invariant curves of figure 15(a) that close around the centre of the island 7, or around the secondary fixed point 14. The maximum Rot $= 0.5057$ appears at the periodic orbit $x = 0.0315$. As x increases the value of Rot decreases, first slowly and then more abruptly and reaches a plateau

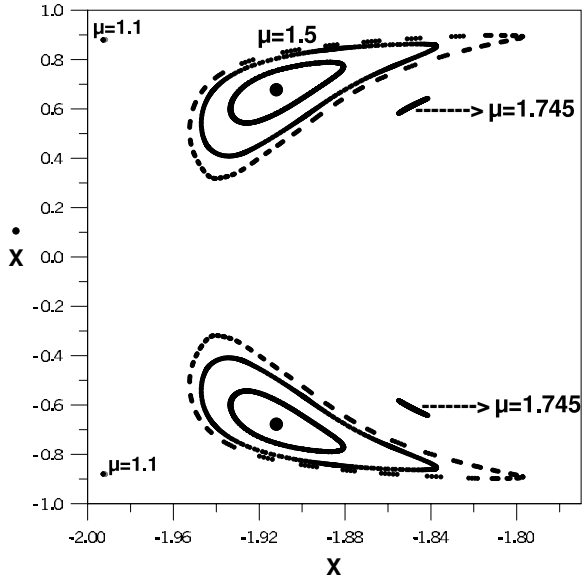

Figure 10. Two islands of stability outside the x-axis around two period 3 points for $\mu = 1.5$ and negative x, and their positions and forms for $\mu = 1.1$ and $\mu = 1.745$.

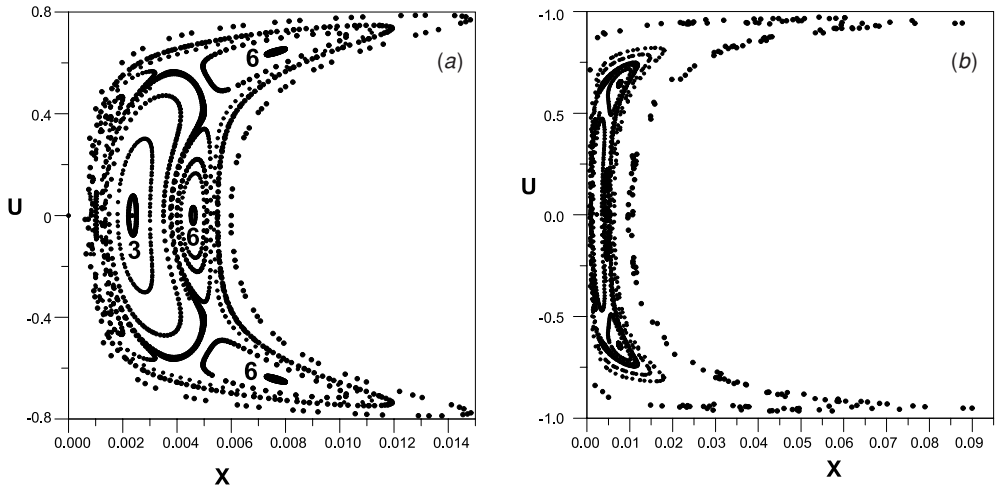

Figure 11. (a) An island of stability of the period-3 orbit for $\mu = 1.3$. In this case there are two couples of secondary islands inside the main island. These islands surround the points of two stable period 6 families that bifurcate from the family 3 for a little larger μ. (b) The same as in figure 11(a) in a larger scale. The maximum invariant curve surrounding the point 3 extends to relatively large distances.

at Rot $= 0.5$, when we have two islands of multiplicity 14 with centres on the x-axis. Two more islands are off the x-axis (figure 15(a)). Beyond these islands the rotation number around the periodic orbit of multiplicity 7 decreases abruptly, reaching Rot $= 0$ at the boundary of the island, near $x \approx 0.037$.

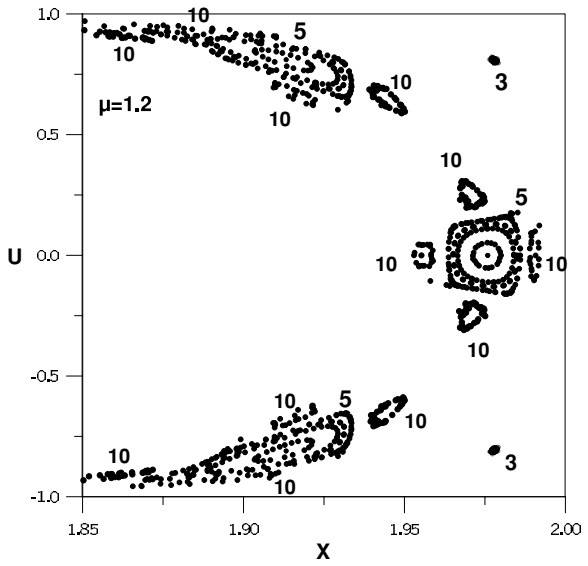

Figure 12. Three islands out of the five islands around a period-5 periodic orbit. Each of them is surrounded by four islands surrounding two stable period 10 periodic orbits. We mark also two points of the period 3 family.

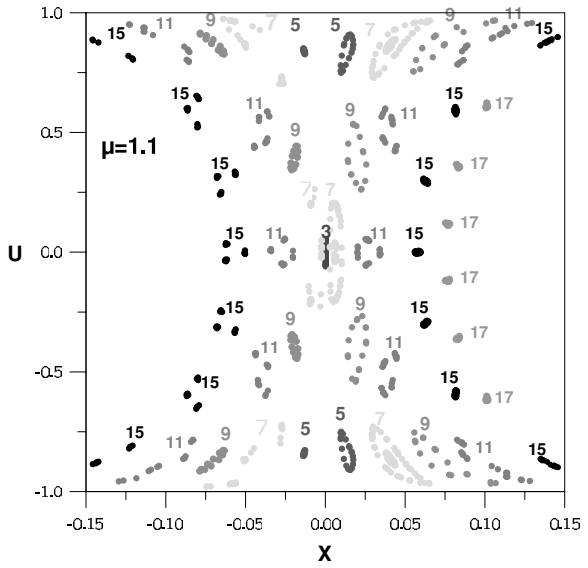

Figure 13. Various islands of stability close to the axis $x = 0$ for $\mu = 1.1$.

7. Asymptotic curves

The asymptotic curves from an unstable periodic orbit give information about the structure of chaos. There are two types of asymptotic curves, the unstable U,UU and the stable S, SS (figures 16–18). The unstable curves never intersect themselves or each other except at

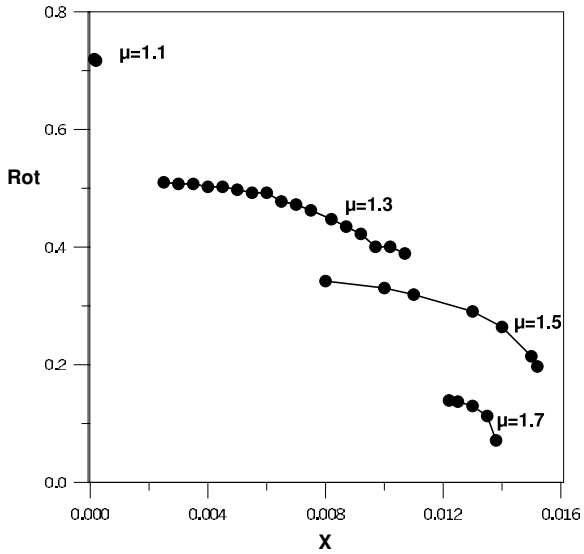

Figure 14. The rotation number around the stable point near the origin, belonging to a stable period 3 orbit for $\mu = 1.1$, $\mu = 1.3$, $\mu = 1.5$ and $\mu = 1.7$.

some singular points that represent collisions with the centre ($x = y = 0$). Similarly the stable asymptotic curves do not intersect themselves or each other.

However, the unstable curves can intersect the stable curves at homoclinic points, if the curves belong to the same periodic orbit, or at heteroclinic points, if the curves belong to different orbits. The homoclinic and heteroclinic orbits are the main characteristics of chaos.

Similar unstable and stable curves can be calculated from every point of the chaotic domain on the surface of section. An example of such curves is given in figure 26 of Gutzwiller (1990) for a mass ratio $\mu = 5$.

All stable and unstable curves reach the lower and upper boundaries (∓ 1) at particular points. These points represent collision orbits, i.e., orbits colliding with the centre ($x = y = 0$).

The collision orbits themselves cannot be extended beyond the collision point. In fact it was shown by Devaney (1978a) that these orbits are not regularizable. However, all other orbits starting on the asymptotic curves have intersection points with the surface of section along the asymptotic curves beyond the collision points.

In figure 16 we have marked various arcs of the asymptotic curves U and S from the central unstable periodic orbit (of period 1) for $\mu = 2$. In particular, the original arc U_1 terminates at a point ($X \approx 1.4$, $U = 1$) on the upper side of figure 16. The next arc U_2–U_3 starts at the left lower side of figure 16, namely at ($X \approx -1.4$, $U = -1$) and reaches the point ($X \approx -0.3$, $U = +1$). Then follows the arc U_4–U_5 on the right, the arc U_6–U_7 on the left, and so on. The arc U_4–U_5 seems to terminate well below the point ($X = 1.4$, $U = +1$). However, if we calculate the asymptotic curve with a much smaller integration step the curve U_4–U_5 extends upwards and tends to ($X = 1.4$, $U = 1$). Similarly the arc U_6–U_7, in fact, starts at ($X = -1.4$, $U = -1$). The reason why a great accuracy is needed is that some orbits come very close to the origin and then a very small step is required.

In the same way, the stable arc S_1 on the right is continued with the arc S_2–S_3 on the left, S_4–S_5 on the right, S_6–S_7 on the left, S_8–S_9 on the right, and so on. Finally we have marked

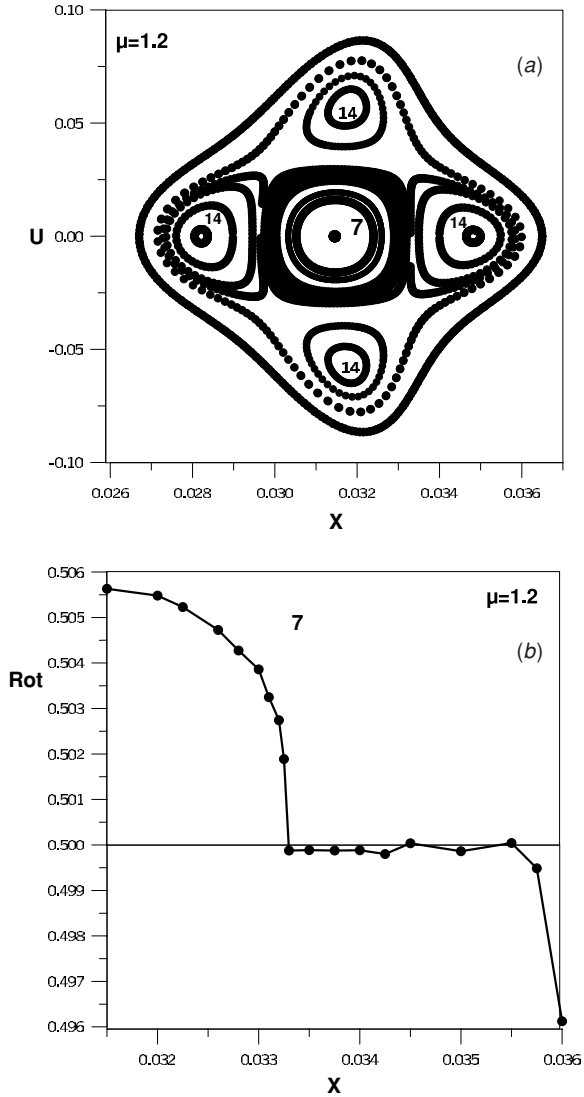

Figure 15. (*a*) One island of period 7 and two islands of period 14 with centres on the x-axis. Two more islands 14 are above and below the periodic orbit 7. Between these islands there are two unstable periodic orbits 14. Island 7 surrounds all four islands of period 14. (*b*) The rotation number Rot around the periodic orbit 7 as a function of the coordinate x of the invariant curves along the $\dot{x} = 0$ axis.

the arcs UU_1 and SS_1 but these arcs also can be continued further with arcs like UU_2–UU_3, SS_2–SS_3, etc.

The original arcs U_1,S_1 do not intersect each other. However, their continuations intersect at infinitely many homoclinic points. For example, the arc U_2–U_3 intersects the arcs S_2–S_3, and S_6–S_7 the arc U_4–U_5 intersects the arcs SS_1 and S_4–S_5, etc.

In figure 17 we have marked a few arcs of the unstable asymptotic curve from the orbit 1 for $\mu = 2$ together with some stable arcs from the unstable orbit $7'''$. We see that there are

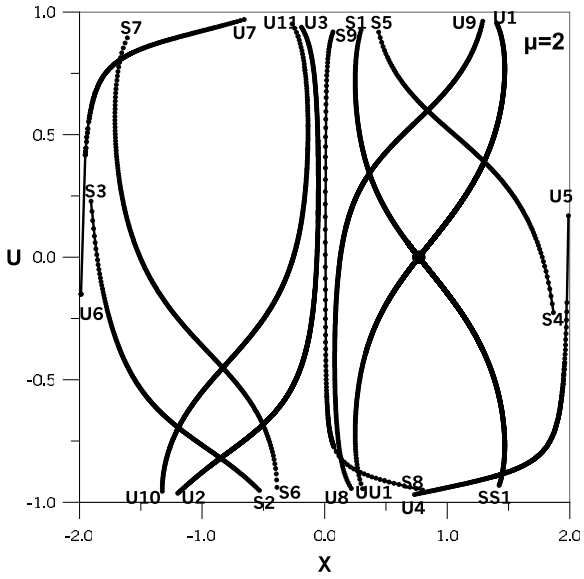

Figure 16. Successive arcs of the unstable (U,UU) and stable (S,SS) asymptotic curves from the unstable periodic orbit 1 for $\mu = 2$. All the arcs start and terminate at particular points on the lines $U = \pm 1$. (The arcs U_4–U_5, U_6–U_7, S_2–S_3 and S_4–S_5 are incomplete). The U and S arcs intersect each other at homoclinic points.

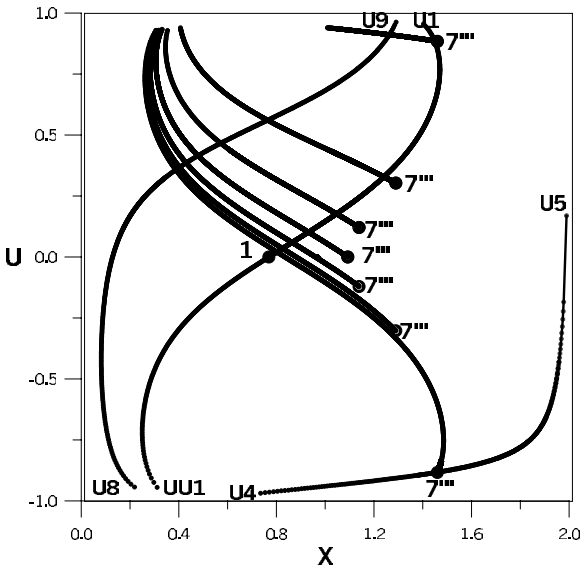

Figure 17. Some unstable arcs of the asymptotic curve of the unstable orbit 1 and some stable arcs of the unstable periodic orbit $7'''$ intersecting at heteroclinic points for $\mu = 2$.

several (in fact infinitely many) heteroclinic intersections between the arcs of the two unstable orbits.

The existence of infinitely many homoclinic and heteroclinic orbits shows that chaos is dominant in the case $\mu = 2$. The curves of figures 16–18 seem to cover completely the whole

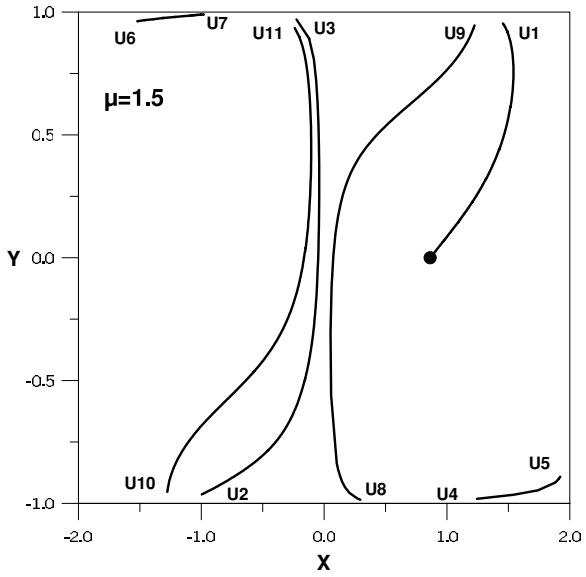

Figure 18. Successive arcs of the asymptotic curve U of the unstable periodic orbit 1 for $\mu = 1.5$. (The arcs U_4–U_5 and U_6–U_7 are incomplete).

phase space on the surface of section. In fact one may think that the empty regions can be filled by similar curves. However, at least for $\mu < 1.748$ there are real empty regions containing islands of stability, as we have discussed in the previous sections. For example, in the case $\mu = 1.5$ (figure 18), the empty regions, containing islands around the stable periodic orbits are given in figures 9 and 10.

Near the homoclinic (and heteroclinic) points there are infinitely many high order periodic orbits (Birkhoff 1927, Danby 1984, Da Silva Ritter *et al* 1987). In the present case we found a periodic orbit of multiplicity 9 close to the homoclinic point (U_1, S_4–S_5) of figure 16 for $\mu = 2$. Then we found periodic orbits of multiplicities 8, 7, 6, 5, 4, 3, 2, starting further away from the homoclinic point. It is obvious that there are infinitely more periodic orbits starting even closer to the homoclinic point. All these orbits are asymmetric with respect to the x-axis, but symmetric with respect to the y-axis. Two orbits of this type are given in figure 19(a) and three orbits are represented on a surface of section (X, U) in figure 19(b). The initial points of these orbits are along a curve starting from the homoclinic point (U_1, S_4–S_5) upwards and to the left (a little above the line S4–S5). As the multiplicity m decreases, the initial points recede from the homoclinic point. In particular, the initial point of the orbit $m = 2$ is rather far from the homoclinic point (U_1, S_4–S_5). The second points of the periodic orbits are close to the homoclinic point (U_2–U_3, S_2–S_3). The third points for $m = 5$ and $m = 9$ are close to the homoclinic point (U_8–U_9, S_1), and the other points are between the first and third points.

All these orbits are highly unstable. Their stability parameters are $a = 4.5$, 10.9, 22.3, 42.0, 75.7, 133.4, 232.2, 400.0 for the orbits of multiplicities $m = 2$, 3, 4, 5, 6, 7, 8, 9, respectively. We note that the stability parameters are almost doubled at each successive orbit.

We notice that the orbits of figure 19(a) are symmetric with respect to the y-axis. Thus they can be found easily because they intersect the x-axis perpendicularly. We calculated many families of orbits of this type for several values of μ, and found that all of them are unstable.

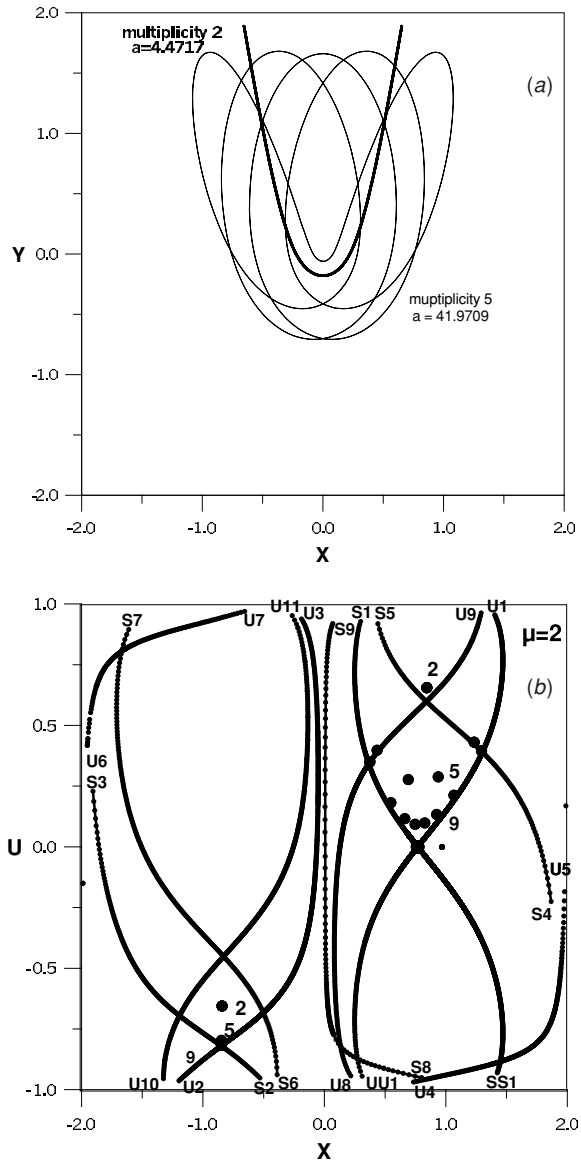

Figure 19. (*a*) Two periodic orbits, of multiplicities $m = 5$ and $m = 2$ (heavy line) for $\mu = 2$ starting close to the homoclinic point (U_1, S_4–S_5) of figure 16. (*b*) Intersections of the periodic orbits of multiplicities $m = 9$, $m = 5$ and $m = 2$ by the surface of section (X, U) together with the asymptotic curves of figure 16.

A question that remains open is whether there are also some small islands of stability of higher order among the stable and unstable asymptotic curves. But even if this is the case, the sizes of such islands are probably extremely small. Therefore we agree with Gutzwiller (1990), who says "The existence of Broucke's island for mass ratios below 2 and presumably other islands that could escape even a high-precision numerical search, seems to exclude any clear-cut and simple mathematical result. Nevertheless, as a physicist, one is tempted to accept that the Anisotropic Kepler Problem behaves effectively like a system with hard chaos". The

only remark that can be added to this statement is that the best way to find any possible islands of stability is by studying the characteristics and stability curves of the various periodic orbits. It is in this way that we have found, beyond the Broucke islands 3 and 5, further islands around the periodic orbits of period 5, 6, 7, 9, 11, 14 and 15, as seen in figure 6.

Gutzwiller (1977), Devaney (1978b), Casasayas and Llibre (1984) and Broucke (1985) developed the theory of the collision orbits on a collision manifold. They introduced two angles θ and Ψ on the collision manifold and found that the flow has a certain spiral form. These calculations allow us to find the positions of the collision points X_c on the axes $U = \pm 1$. For mass ratios $\mu > 9/8$ there are infinitely many collision points, while for $\mu < 9/8$ there is only a finite number of such points.

By comparing figures 16 and 18 for $\mu = 2$ and $\mu = 1.5$, figure 26 of Gutzwiller (1990) for $\mu = 5$ and data for $\mu = 20$, we see that the collision values of $|X_c|$ increase in general as μ decreases. Most of the values of $|X_c|$ are close to +2.

8. Conclusions

The anisotropic Kepler problem (AKP) is particularly intriguing because it does not have the usual structure of dynamical systems generated by introducing a smooth perturbation in an integrable system. In such systems the unperturbed system has one or more stable periodic orbits that remain stable in the perturbed system; chaos appears near the unstable periodic orbits, and it becomes larger as the perturbation increases. But in the AKP the main periodic orbit of the Kepler problem (the circular orbit of period 1) becomes unstable with the slightest perturbation. The other periodic orbits of the Kepler problem disappear altogether and the topology of the periodic orbits of the AKP is quite different from that of the Kepler problem. The reason is that the perturbation for μ different from 1 is not small but large close to the origin.

In previous studies of the AKP the emphasis was given on the chaotic orbits, particularly on the asymptotic orbits and the collision orbits.

In the present paper, on the contrary, we applied a number of methods used in general dynamical systems, and found several new results.

(1) We found several families of stable periodic orbits (up to order 17) and their regions of stability, by calculating the invariant curves of orbits trapped around them.

(2) As the anisotropy index μ tends to 1 (Kepler problem), the positions of most periodic orbits tend in general either to $x = 0$ (origin), or to $|x| = 2$ (boundary). Only the orbit of period 1 (circular orbit of the Kepler problem) tends to $x = 1$.

(3) The stability parameter α of the stable orbits is between -1 and 1. As μ tends to zero, it seems that α tends to +1 or to -1. However, there are several completely unstable families, whose stability parameter α increases as μ tends to 1 and goes presumably to $\alpha = \infty$. As μ increases along these families, the value of α first decreases to a minimum, above $\alpha = 1$, and then increases as μ increases further.

(4) All the families that we have found become unstable for a large enough μ. The largest μ for which we have found a stable family (of period 3) is $\mu = 1.748$. However, we conjecture that there are higher-order stable families for even larger μ.

(5) When the stability curve (α versus μ) crosses the line $a = 1$ at a certain value $\mu = \mu_C$, we have the bifurcation of a new family. But such families are in general unstable and exist only for $\mu < \mu_C$. Thus they are unstable and they do not generate new stable families for larger μ. In two cases (families 11 and 15), we have at one point bifurcation of a

stable family. But this family exists only up to another bifurcation point and terminates there.

(6) Most of the stability curves touch the line $a = -1$, but do not cross this line. At the tangent point we have the bifurcation of two double period stable families (and two unstable families), but these families exist for smaller μ. Only in one case (family 14) the stability curve goes below the line $a = -1$ but only in a small interval of values of μ.

(7) The stability regions (islands) around every stable periodic orbit are defined by the largest closed invariant curve around the periodic orbit on a Poincaré surface of section. For small μ (but $\mu > 1$), there are many islands of stability (figure 13).

(8) We have calculated the rotation number Rot of various invariant curves around some stable periodic orbits as a function of x. Rot is maximum at the periodic orbit and it tends to zero at the boundary of the island. As Rot passes through rational values, we find some intervals of x where Rot is a constant rational n/m, and there we have bifurcated islands.

(9) The maximum Rot is largest for small μ, but the extent of the islands is very small for μ close to 1 and also for μ close to the maximum stable value of every family. In the case of family 3 the largest island appears close to $\mu = 1.5$.

(10) In all cases with $\mu > 1$ there is chaos. The degree of chaos is given by calculating the maximal LCN. The finite time LCN χ (equation (12)) tend to the same LCN for all the orbits outside the islands when $t \to \infty$, while they tend to LCN $= 0$ for the invariant curves inside the islands.

(11) We have calculated the value of LCN as a function of μ. LCN increases from zero (at $\mu = 1$) to a maximum value close to LCN $= 0.21$ at $\mu = 4$, and then decreases continuously. For $\mu = 100$, the value of LCN is about LCN $= 0.10$. It seems that LCN $\to 0$ as μ tends to infinity. On the other hand, there is no discontinuity when $\mu = 9/8$, despite some claims that there is no chaos for $\mu < 9/8$.

(12) The finite time LCN χ increases locally when an orbit approaches the origin, but beyond such an approach the value of χ levels off close to its final value LCN.

(13) The asymptotic curves from the unstable periodic orbits on a surface of section reach certain 'collision points' X_c on the lines $U = \pm 1$ but they continue beyond these points. Namely, if an asymptotic curve reaches the line $U = +1$ it continues from a point on the line $U = -1$. Thus the asymptotic curves are composed of an arc from the periodic orbit to one of the limiting lines $U = \pm 1$, and are continued with arcs from $U = -1$ to $U = +1$.

(14) The stable and unstable asymptotic curves intersect at an infinity of homoclinic and heteroclinic points. The corresponding homoclinic and heteroclinic orbits are the main manifestations of chaos.

(15) Close to every homoclinic and heteroclinic orbit are the initial conditions of infinitely many periodic orbits. We found several periodic orbits of this type, but all of them are unstable. In fact the stability parameter of a periodic orbit almost doubles at each successive multiplicity.

Acknowledgment

This work was supported by the Research Committee of the Academy of Athens.

Appendix. Definitions of various terms

The definitions of the technical terms in the present paper can be found in standard textbooks (e.g. Lichtenberg and Lieberman 1992, Contopoulos 2004). However, to facilitate a quick reference we give some definitions and descriptions here.

A.1. Anosov system

A system having everywhere a positive Lyapunov characteristic number between two fixed limits

$$C_1 \leqslant LCN \leqslant C_2. \tag{A.1}$$

Such a system is completely chaotic, e.g. it does not have any stable periodic orbits.

A.2. Bernoulli system

A system isomorphic to a map generated by shifting (to the left) the dot separating two binary numbers $x = \cdot a_1a_2a_3\ldots$ and $y = \cdot b_1b_2b_3\ldots$ written in the form

$$\ldots b_3b_2b_1 \cdot a_1a_2a_3\ldots \tag{A.2}$$

Namely, the map is $(x, y) \rightarrow (x', y')$, with $x' = \cdot a_1'a_2'a_3'\ldots . y' = \cdot b_1'b_2'b_3'\ldots$ and $b_i' = b_{i+1}$ $(i \geqslant 1)$, $a_1' = b_1$, $a_i' = a_{i-1}$ $(i \geqslant 2)$. A Bernoulli system is a paradigm of an Anosov system.

A.3. Standard map

The map

$$x' = x + y', \qquad y' = y + \frac{K}{2\pi}\sin(2\pi x) \pmod 1 \tag{A.3}$$

where K is the perturbation parameter.

A.4. Stability parameter

A parameter determining the stability or instability of a periodic orbit (e.g. Hénon 1965). In a two-dimensional map $(x, y) \rightarrow (x', y')$ a small deviation $(\Delta x_0, \Delta y_0)$ from a periodic orbit is mapped at $(\Delta x_1, \Delta y_1)$, where

$$\Delta x_1 = a\Delta x_0 + b\Delta y_0, \qquad \Delta y_1 = c\Delta x_0 + d\Delta y_0. \tag{A.4}$$

If the map is conservative the determinant of the monodromy matrix is $ad - bc = 1$ and the eigenvalues λ satisfy the equation

$$\lambda^2 - (a + d)\lambda + 1 = 0. \tag{A.5}$$

If $|a + d| > 2$ the eigenvalues $\lambda_1, \lambda_2 = 1/\lambda_1$ are real and the periodic orbit is unstable, while if $|a + d| < 2$ the eigenvalues are complex and the orbit is stable.

The stability parameter is $(a + d)/2$. If the orbit is symmetric we have $a = d$ and the stability parameter is equal to a. If $|a| > 1$ the orbit is unstable and if $|a| < 1$ it is stable.

A.5. Invariant curve

In a two-dimensional map a curve whose points have images on the same curve is an invariant curve. This curve can be closed (around a stable periodic orbit), or open.

A.6. Asymptotic curves

A map close to an unstable periodic orbit (x_0, y_0) defines two eigenvectors forming angles Φ_i $(i = 1, 2)$ with the x-axis, where

$$\tan \Phi_\iota = \frac{\lambda_i - a}{b} \tag{A.6}$$

λ_i are the roots of equation (A.5), and a, b are the parameters of the first equation (A.4).

The asymptotic curves are invariant curves containing the points whose images or pre-images approach asymptotically the period orbit. The asymptotic curves are tangent to the eigenvectors at (x_0, y_0) but further away they deviate from the eigenvectors. There are two unstable asymptotic curves, corresponding to $\lambda_1 > 1$, one opposite to the other, along which the images (x', y') of points (x, y) recede from (x_0, y_0), and two stable asymptotic curves, corresponding to $\lambda_2 = 1/\lambda_1 < 1$, again one opposite the other, along which the images (x', y') of the points (x, y) approach the periodic orbit (x_0, y_0).

A.7. Homoclinic and heteroclinic points

The asymptotic curves are closed only in integrable systems, while in nonintegrable systems they are open. An unstable asymptotic curve does not intersect itself or any other unstable asymptotic curve. Similarly a stable asymptotic curve does not intersect itself or another stable asymptotic curve. However, an unstable asymptotic curve may intersect one or both stable asymptotic curves from the same periodic orbit at infinitely many 'homoclinic points'. It may intersect also the stable asymptotic curves of other periodic orbits at infinitely many 'heteroclinic points'. The homoclinic points have images that approach asymptotically the same periodic orbit in the future and in the past, while the heteroclinic points have images that approach asymptotically the original periodic orbit in the past (pre-images) and another periodic orbit in the future.

A.8. Regularizable and nonregularizable orbits

This term characterizes orbits that reach a singular point of the potential. Such is a straight line orbit in the Kepler problem. If there is a transformation of the coordinates and of the time that transforms the collision point into a nonsingular point of the orbit this orbit is regularizable, while if this is impossible the orbit is nonregularizable (Devaney 1978a).

References

Bai Z-G and Zheng W-M 2002 *Phys. Lett.* A **300** 259
Birkhoff G D 1927 *Acta Math.* **50** 359
Bunimovich L A and Sinai Ya G 1980 *Commun. Math. Phys.* **78** 247
Broucke R 1985 *Dynamical Astronomy* ed V G Szebehely and B Balazs (Austin, TX: Univiversity of Texas Press) p 9
Casasayas J and Llibre J 1984 *Memoirs of the American Mathematical Society* vol 312 (Providence, RI: American Mathematical Society)
Contopoulos G 2004 *Order and Chaos in Dynamical Astronomy* (New York: Springer)
Dahlquist P and Russberg G 1990 *Phys. Rev. Lett.* **65** 2837
Danby J M A 1984 *Celest. Mech.* **33** 261
Da Silva Ritter G L, Ozorio de Almeida A M and Douady R 1987 *Physica* D **29** 181
Devaney R L 1978a *J. Diff. Eqns* **29** 253
Devaney R L 1978b *Inventory Math.* **45** 221
Gutzwiller M C 1967 *J. Math. Phys.* **8** 1979
Gutzwiller M C 1969 *J. Math. Phys.* **10** 1004
Gutzwiller M C 1970 *J. Math. Phys.* **11** 1791

Gutzwiller M C 1971 *J. Math. Phys.* **12** 343
Gutzwiller M C 1974 *J. Math. Phys.* **14** 139
Gutzwiller M C 1977 *J. Math. Phys.* **18** 806
Gutzwiller M C 1982 *Classical Mechanics and Dynamical Systems* ed R L Devaney and Z Nitecki (New York: Marcel Decker) p 69
Gutzwiller M C 1989 *Physica* D **18** 160
Gutzwiller M C 1990 *Chaos in Classical and Quantum Mechanics* (New York: Springer)
Hénon M 1965 *Ann. Astrophys.* **28** 992
Lichtenberg A J and Lieberman M A 1992 *Regular and Chaotic Dynamics* 2nd edn (New York: Springer)